The somatostatin analogue octreotide inhibits capsaicin-mediated activation of nociceptive primary afferent fibres in spinal cord lamina II (substantia gelatinosa)

The somatostatin analogue octreotide inhibits capsaicin-mediated activation of nociceptive primary afferent fibres in spinal cord lamina II (substantia gelatinosa)

Ileana Bencivinni [a], Francesco Ferrini [a], Chiara Salio [a], Massimiliano Beltramo [b], Adalberto Merighi [a,c]

[a] Department of Veterinary Morphophysiology, Via Leonardo da Vinci 44, 10095 Grugliasco, Italy

[b] Institut National de la Recherche Agronomique, UMR0085, Physiologie de la Reproduction et de Comportements, 37380 Nouzilly, France

[c] Istituto Nazionale di Neuroscienze (INN), Università degli studi di Torino, Corso Raffaello 30, 10125, Torino, Italy

Abstract

Somatostatin (SST) in spinal cord has been linked with the inhibition of nociceptive neurotransmission in several experimental paradigms. The SST2 receptor (SSTR2) is the main SST receptor subtype in the superficial dorsal horn (DH) and is activated, besides to the naïve peptide, by the SST synthetic analogue octreotide (OCT). In the present work, we have studied the central effects of SSTR2 activation on capsaicin (CAP)-induced glutamate release in mouse DH. In neurons of the lamina II of DH, CAP (2 μM) induced a strong increase of mEPSC frequency that was significantly reduced (70%) by OCT. SSTR2 involvement was assessed by using the specific antagonist CYN 154806. No differences were observed between frequency increase in CAP alone vs. CAP in the presence of CYN 154806 + OCT. The effect of OCT was further investigated by studying c-fos expression in spinal cord slices. The CAP-induced increase in density of Fos immunoreactive nuclei in the superficial DH was strongly prevented by OCT.

SSTR2a (a splicing variant of SSTR2) immunoreactivity was found in both pre- and post-synaptic compartments of laminae I–II synapses. By light and electron microscopy, SSTR2a was mainly localized onto non-peptidergic isolectin B4 (IB4)-positive primary afferent fibres (PAFs). A subset of them was also found to express the CAP receptor TRPV1.

These data show that the SST analogue OCT inhibits CAP-mediated activation of non-peptidergic nociceptive PAFs in lamina II. Our data indicate that SSTR2a plays an important role in the pre-synaptic modulation of central excitatory nociceptive transmission in mouse.

Key words: capsaicin, octreotide, SST2 receptors, dorsal horn, nociception

Corresponding author at: Department of Veterinary Morphophysiology, Via Leonardo da Vinci 44, 10095 Grugliasco (TO), Italy. Tel.: +39 0116709118; fax:

+39 0112369118.
E-mail address: adalberto.merighi@unito.it (A. Merighi).

1. Introduction

Somatostatin (SST) is a small peptide widely distributed in brain and peripheral tissues. SST can be detected in several areas of the central nervous system (CNS), including the spinal cord, where it exhibits a variety of physiological effects (Selmer et al., 2000; Viollet et al., 2008) by binding to a specific group of G-protein coupled receptors (Patel and Srikant, 1997; Olias et al., 2004). These latter have been cloned and characterized, eventually leading to the discovery of five different molecules (referred to as SSTR1-5) that have been collected into two main families on the basis of structural and functional features (Viollet et al., 1995; Patel, 1999). The effects of SST in spinal cord are usually associated with an inhibition of nociceptive neurotransmission in several experimental paradigms (Carlton et al., 2001; Su et al., 2001; Malcangio et al., 2002), and the peptide, as well as its synthetic analogue octreotide (OCT), have been shown to evoke analgesia in many clinical situations, including several different types of pathological pain (Penn et al., 1992; Paice et al., 1996; Dahaba et al., 2009).
Morphological studies in rat have shown that SST and SSTRs are expressed in primary afferent fibres (PAFs) and neurons in the spinal cord dorsal horn (DH; Segond Von Banchet et al., 1999), as wells as in dorsal root ganglia (DRGs; Bar et al., 2004), these anatomical localization being supportive of the role of the peptide in the control of nociceptive information.
More precisely, SSTR2a is contained in a dense network of processes as well as in small round neuronal cell bodies within the superficial DH, whereas SSTR2b is prominent throughout the spinal grey matter in the somas and proximal dendrites of relatively large neurons (Schulz et al., 2000). In DRGs, expression of SSTR1-4 receptors has been shown in small and large sized cell bodies (Bar et al., 2004; Señaris et al., 1995).

Electrophysiological studies in rat so far have only reported post-synaptic SST-induced hyperpolarisation in a sub-population of DH neurons, and, in general, have failed to show any significant SST-mediated pre-synaptic effect at PAF central endings (Kim et al., 2002; Jiang et al., 2003).
Carlton and colleagues (2004) have demonstrated that the activation of SSTR2 expressed peripherally on rat PAFs reduces the pro-nociceptive effects of capsaicin (CAP), the pungent vanilloid of hot chili pepper (Caterina et al., 1997; Tominaga et al., 1998). Given that the CAP receptor, TRPV1 is also highly expressed in the central projections of nociceptive neurons giving rise to C and Ad PAFs (Michael and Priestley, 1999; Guo et al., 2001), one may hypothesize that SST also modulates the central effects of the vanilloid. These latter are mainly due to CAP-induced neurotransmitter release (Urban and Dray, 1992; Yang et al., 1998; Ferrini

et al., 2007) at the synapse between PAFs and DH neurons.
In this paper, we devised a series of experiments to assess whether or not activation of mouse pre-synaptic SSTR2a in lamina II of the DH may challenge the effects of TRPV1 on spinal excitatory neurotransmission.

2. **Methods**

All experimental procedures were approved by the Italian Ministry of Health and the Committee of Bioethics and Animal Welfare of the University of Torino. Animals were maintained according to NIH Guide for the Care and Use of Laboratory Animals.

2.1. **Electrophysiology**

Post-natal CD1 mice (P8-P12; n = 29) were deeply anaesthetized with an intraperitoneally administered lethal dose of sodium pentobarbital (30 mg/kg). The thoracic and lumbar regions of the spinal cord were removed and constantly maintained submerged in ice-cold artificial cerebro-spinal fluid (ACSF) containing: NaCl 125 mM, KCl 2.5 mM, $NaHCO_3$ 25 mM, NaH_2PO_4 1 mM, glucose 25 mM, $MgCl_2$ 1 mM, $CaCl_2$ 2 mM, saturated with 95% O_2-5% CO_2 during the entire procedure. Three hundred and fifty micrometer-thick coronal slices were cut with a vibrating microtome. Slices were allowed to recover in oxygenated ACSF at 35 °C for at least 30 min and maintained at room temperature until use. During recording slices were constantly perfused (2 ml/min) with oxygenated ACSF. Lamina II neurons were visually identified with a fixed stage upright microscope (Axioskop 1, Zeiss, Göttingen, Germany) equipped with infrared gradient contrast optics (Luigs and Neumann, Ratingen, Germany) using a 40x water immersion objective (Achroplan, Zeiss, Göttingen, Germany). Patch pipettes were obtained from single-filament borosilicate capillaries (WPI, Berlin, Germany) using a vertical puller (PC-10; Narishighe, Tokyo, Japan), and their resistances ranged from 4 to 7 MX once filled with the intracellular solution.
Miniature excitatory post-synaptic currents (mEPSCs) were recorded with a low chloride intracellular solution, containing: $CsMeSO_4$ 145 mM, EGTA 5 mM, $MgCl_2$ 2 mM, HEPES 10 mM, ATP.-Na 2 mM and 0.1% Lucifer Yellow (LY; Sigma Chemicals, St. Louis, MO, USA) pH 7.2 (with CsOH). Guanosine 5’ -[b-thio]diphosphate (GDP-b-S; 1 lM) was added to the pipette to competitively inhibit the binding of GTP by G-proteins and prevent post-synaptic effects mediated by SST receptors. mEPSCs were isolated in presence of tetrodotoxin (TTX; 1 μM) at the holding potential of -65 mV.
Whole-cell patch-clamp recordings were obtained with an Axopatch 200B amplifier (Molecular Devices, Foster City, CA, USA), sampled at 10 kHz and filtered at 2 kHz. Analysis was performed off-line with Minianalysis software (Synaptosoft Inc., Decatur, GA, USA).

Recordings were included for subsequent analysis only if access resistance was stable throughout the recording session.
For data analysis, amplitude and frequency of mEPSCs in control traces and after CAP application were compared within 200s time intervals, using the Kolmogorov–Smirnov test for statistical significance. Neurons were classified as responsive when the distribution of inter-event interval and/or amplitude values following CAP administration were significantly different compared to the control ($P < 0.01$).
Pooled data were reported as mean ± SEM, with n indicating the number of neurons. Wilcoxon matched-pairs test was used to com- pare frequency and amplitude values of grouped neurons ($P < 0.05$).
Differences between normalized data (expressed as a percent- age of the predrug control value ± SEM) were analyzed with Kruskal–Wallis test and Dunn's test post hoc. Data were considered significantly different when $P < 0.05$.
All drugs were bath applied. CAP, OCT, CYN 154806 and TTX were from Tocris (Bristol, UK). All other drugs were purchased from Sigma Chemicals. CAP was used at 2 μM final concentration (Ferrini et al., 2007). CYN 154806 has recently been proved to be effective in blocking mouse SSTR2 in vivo (Terashima et al., 2009). The antagonist was used on slices at 1 μM final concentration on the basis of slice experiments in rat (Mori et al., 2010) and mouse (Cammalleri et al., 2004). The same concentration was also effective in blocking SSTR2 in cultured rat trigeminal ganglion neurons (Takeda et al., 2007) and in CHO-K1 cell membranes expressing recombinant hu- man SSTR2 or rat SSTR2a and b (Feniuk et al., 2000).

2.2. Light and electron microscopy

All immunohistochemical studies were carried out on P8-12 (n = 4) and P21-23 (n = 4) CD1 mice. The reason for studying post-natal mice at different ages is be- cause nociceptive circuits are subjected to substantial post-natal functional maturation, particularly as regarding to C fibres activity (see Fitzgerald, 2005), which is completed around the third post- natal week in rat/mouse. Nonetheless, we have recently shown that the response to CAP is unchanged in slices obtained from P8-12 or P21-23 mice (Ferrini et al., 2010). Given that healthy slices are more easily obtained from more juvenile mice, we wanted to make ourselves sure that there were no obvious differences in expression of SSTR2a in these animals hampering electro- physiological studies.
Under deep pentobarbital anaesthesia, mice were perfused through the descending aorta with Ringer solution, followed by cold fixative. The latter consisted of 4% paraformaldehyde in 0.2 M phosphate buffer (PB) for light microscopy and 4% paraformaldehyde +0.01% glutaraldehyde for electron microscopy. After perfusion, the lumbar spinal cord was cut in segments, and, after careful dissection, post-fixed for 2 additional hours in the same aldehyde mixture. Coronal sections were cut on a vibratome at a thickness of 70 μm.

The following primary antibodies have been used: goat-anti- SSTR2a (1:100 – Santa Cruz, Biotechnology, Santa Cruz, CA), rabbit anti-SST (1:1000 – raised against SST-28; Merighi et al., 1989), rab- bit anti-CGRP (1:1000 – Merighi et al., 1991), rat anti-SP (1:500 – BD Pharmingen, Franklin Lakes, NJ, USA), rabbit anti-TRPV1 (1:1000 – Alomone Labs, Jerusalem, Israel), rabbit anti-Fos (1:100 – Abcam, Cambridge, UK). Lectin from Bandeiraea simplicifolia (Griffonia simplicifolia), biotin conjugated (IB4; 1:250 – Sigma Chemicals) was also used in immunohistochemical procedures.

The anti-SSTR2a antibody was raised against a specific sequence at C terminus of human SSTR2 that shares 100% homology with the mouse SSTR2a (Møller et al., 2003). This sequence is lacking in the mouse SSTR2b, a truncated isoform of the receptor (Møller et al.,2003), and is totally unrelated to the sequences of mouse SSTR1 (Yamada et al., 1992), SSTR3 (Yasuda et al., 1992), SSTR4 (Schwabe et al., 1996) and SSTR5 (Baumeister et al., 1998).

Immunocytochemical controls consisted in omission of primary antibodies. Double immunofluorescence stainings were performed by rou- tine procedures as described elsewhere (Ferrini et al., 2007, 2010). Immunofluorescence was acquired using a Leica TCS SP5 confocal laser scanning microscope. Green and red fluorescence were then merged using Photoshop 7.0.1 (Adobe Systems, San Jose, CA, USA).

Pre-embedding immunostaining for SSTR2a visualization at the electron microscope was performed with Fluoronanogold™- Streptavidin (Nanoprobes, Yaphank, NY, USA) as described previ- ously (Salio et al., 2005).

2.3. **Fos response to slice functional stimulation**

Fos activation was studied in spinal cord slices as previously de- scribed (Vergnano et al., 2008). Briefly, spinal cord acute slices were obtained from two P8-12 CD1 mice and subjected to one of the following experimental treatments: (i) maintenance in ACSF for 3 h (control); (ii) incubation with CAP 2 μM for 10 min and then washing in ACSF for 3 h (CAP); (iii) pre-incubation with OCT 1 μM for 30 min, then incubation with CAP and washing as above in constant presence of OCT (CAP + OCT). Slices were then fixed, embedded in paraffin wax and processed for DAB immunocytochemistry. Immunostained sections were photographed with a 20x objective.

The boundaries of the dorsal horn laminae were delineated according to criteria set by Molander et al. (1984) and Paxinos and Watson (1998). The cell density (number of cells/mm^2) within the superficial DH (laminae I–II) was calculated with the ImageJ software (NIH, Bethesda, Maryland, USA). Analysis was performed blind to the treatment. Statistics was performed with one-way ANOVA (Bonferroni post hoc, $P < 0.05$). Data were expressed as mean ± SEM, with n indicating the number of DH slices examined.

3. **Results**

3.1. **Effects of OCT on mEPSCs after CAP pulses**

The effect of OCT was studied after specific pre-synaptic activation of nociceptive pathways by CAP. Pre-synaptic effects were isolated by blocking post-synaptic SSTRs with a competitive G protein inhibitor dissolved in the recording pipette (GDP-b-S, 1 mM) and by bath-application of TTX (1 μM) to block action potential-mediated neurotransmission. All tested neurons were responsive to CAP application with a significant increase of mEPSCs frequency (Kolmogorov–Smirnov test, $P < 0.01$).

In lamina II neurons, incubation with CAP (2 μM – 1 min, Fig. 1A) induced a strong increase in mEPSCs frequency from 0.36 ± 0.09 Hz to 12.89 ± 3.35 Hz ($n = 7$, Wilcoxon test, $P < 0.05$, Fig. 1D, white bars). A small increase in mEPSC amplitude was observed in only 3 out of 7 neurons (Kolmogorov–Smirnov test, $P < 0.01$), mainly due to a relative increase of large mEPSCs after capsaicin; however the overall change in the mean amplitude was not significant (con- trol: 39.29 ± 8.79 pA, CAP: 40.37 ± 6.45 pA, Wilcoxon test, $P > 0.05$, Fig. 1E, white bars). When the same experiment was performed in presence of OCT (Fig. 1B), CAP induced a smaller (albeit still significant) increase of frequency compared to control (from 1.01 ± 0.35 Hz to 5.94 ± 2.08 Hz, $n = 8$, Wilcoxon test, $P < 0.05$, Fig. 1D, black bars). Similarly to the observations made after CAP alone, mEPSC amplitude was increased in only 4 out of 8 neurons (Kolmogorov–Smirnov test, $P < 0.01$), but not in the pooled data (control: 23.52 ± 1.91 pA, CAP + OCT: 26.93 ± 3.16 pA, $n = 8$, Wilcoxon test, $P > 0.05$, Fig. 1E, black bars). To investigate any possible involvement of SSTR2, a third series of experiments was per- formed in presence of CYN 154806, a specific SSTR2 antagonist (1 μM; Cammalleri et al., 2004; Takeda et al., 2007), and OCT (Fig. 1C). In presence of CYN 154806+OCT (Fig. 1C), CAP induced an increase of mEPSC frequency (from 0.85 ± 0.19 Hz to 10.69 ± 3.03 Hz $n = 10$, Wilcoxon test, $P < 0.05$, Fig. 1D, grey bars) as well as in amplitude (from 24.06 ± 1.36 pA in control to 31.96 ± 2.74 pA, Wilcoxon test, $P < 0.05$, Fig. 1E, grey bars).

To allow comparisons of the CAP effects under the above experimental conditions, we normalized electrophysiological data following the CAP pulse with their own controls (Fig. 2). As evidenced in Fig. 2A–C, normalized data turned out to give an accurate estimate of the CAP effect under different pharmacological conditions. The frequency increase induced by CAP alone (4032.86 ± 932.47%, $n = 7$, Fig. 2D, white bar) was significantly more intense than the effect of CAP in the presence of OCT (1087.75 ± 455.10%, $n = 8$, Kruskal–Wallis test with Dunn's post hoc test, $P < 0.05$, Fig. 2D, black bar). Conversely, no differences were observed between frequency increase in CAP alone vs. CAP in presence of CYN 154806+OCT

(2296.40 ± 956.54%, n = 10, Kruskal–Wallis test with Dunn's post hoc test, P > 0.05, Fig. 2D, grey bar). No differences were observed among normalized mEPSC amplitude values (CAP: 109.57 ± 8.51%, Fig 2E, white bar, CA- P + OCT: 113.12 ± 5.88%, Fig. 2E, black bar, CAP + OCT + CYN 154806: 132.30 ± 8.28%, Kruskal–Wallis test with Dunn's post hoc test, P > 0.05, Fig. 2E, grey bar).

In brief, these observations indicate that OCT administration pre-synaptically reduces the effect of CAP by about 70%, and that this reduction is largely mediated by SSTR2 activation.

3.2. Distribution of SSTR2a immunoreactivity in DH

Since our electrophysiological findings suggested that the effect of OCT on CAP-induced activation of nociceptive PAFs was pre- synaptic, and previous studies have reported a prevalent localization of the receptor subtype SSTR2a in DRGs (Schulz et al., 1998b; Carlton et al., 2004), we used a primary antibody specifically raised against this receptor isoform for histological localization experiments. The distribution of SSTR2a was studied in P8-12 and P21-23 CD1 mice at both light and electron microscope (see Section 3.2 and Fig. 4) levels. No differences were observed, thus showing that SSTR2a is not subjected to any obvious postnatal regulation in nociceptive circuits.

3.2.1. Light microscopy

SSTR2a immunoreactivity was exclusively found in the superficial laminae of DH. A very dense plexus of processes was distributed in laminae I and II, with no immunoreactive cell bodies.

In order to better characterize the type(s) of neuronal processes displaying SSTR2a immunoreactivity, we carried out a series of double labelling immunofluorescence experiments at the confocal microscope, using different markers of non-peptidergic (IB4) and peptidergic (SP, CGRP, SST) nociceptive PAFs. These experiments revealed that SSTR2a was mainly expressed in a population of IB4 non-peptidergic nociceptive PAFs (Fig. 3A). Examination of SSTR2a + SP (Fig. 3B) and SSTR2a + CGRP (Fig. 3C) immunostained preparations confirmed that there were no SSTRs2a in peptidergic nociceptive PAFs, being the two markers completely segregated in two different populations of processes. Finally, a subset of SSTRs2a were at times co-expressed with SST in some neuronal processes within lamina II (Fig. 3D).

We then studied the relation between SSTR2a and TRPV1, the vanilloid receptor activated by CAP and expressed by a class of PAFs specifically involved in nociception.

In a first series of double immunofluorescence experiments we confirmed that TRPV1 was expressed by both peptidergic and non-peptidergic PAFs of laminae I–II$_O$, these two types of processes respectively expressing SP (Fig. 3E) or IB4 (Fig. 3F).

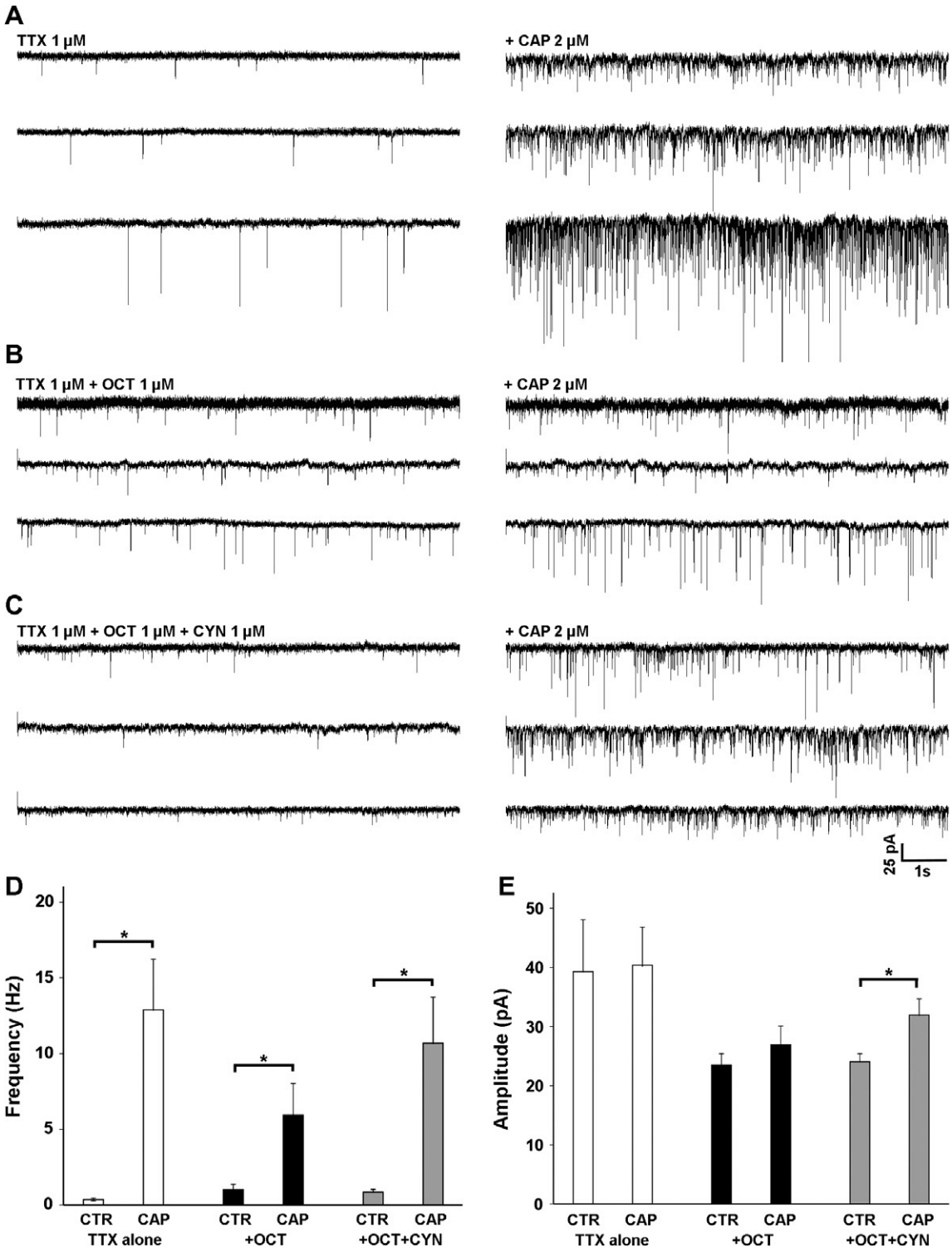

Fig. 1. Effects of OCT on mEPSC after CAP pulses (1 min, 2 µM). (A–C) Representative traces of mEPSC frequency increase in steady presence of TTX 1 µM (A), TTX 1 µM + OCT 1 µM (B), or TTX 1 µM + OCT 1 µM + SSTR2 antagonist CYN 154806 1 µM (C). V_h = - 65 mV. (D) Effect of CAP on mEPSC frequency in the presence of TTX (white bars; n = 7, Wilcoxon matched-pairs test, $^*P < 0.05$), TTX + OCT (black bars; n = 8, Wilcoxon matched-pairs test, $^*P < 0.05$), or TTX + OCT + CYN 154806 (grey bars, n = 10, Wilcoxon matched-pairs test, $^*P < 0.05$).(E) Effect of CAP on mEPSC amplitude in the presence of TTX (white bars; n = 7, Wilcoxon matched-pairs test, $P > 0.05$), TTX + OCT (black bars; n = 8, Wilcoxon matched-pairs test, $P > 0.05$), or TTX + OCT +

CYN 154806 (grey bars, n = 10, Wilcoxon matched-pairs test, *P < 0.05). Abbreviations: CTR, control; CAP, capsaicin; OCT, octreotide; CYN, CYN 154806.

Then, SSTR2a + TRPV1 immunostained preparations revealed a co- expression of the two receptors in fibres localized at the border between lamina II_o and lamina II_i (Fig. 3G).

3.2.2. **Electron microscopy**

The ultrastructural distribution of SSTR2a was examined using a pre-embedding fluoronanogold staining protocol. By this approach, SSTR2a immunoreactivity was found in both pre- and post-synaptic compartments of laminae I–II synapses, with immunolabelling in terminals (Fig. 4A and B) and dendrites (Fig. 4C).

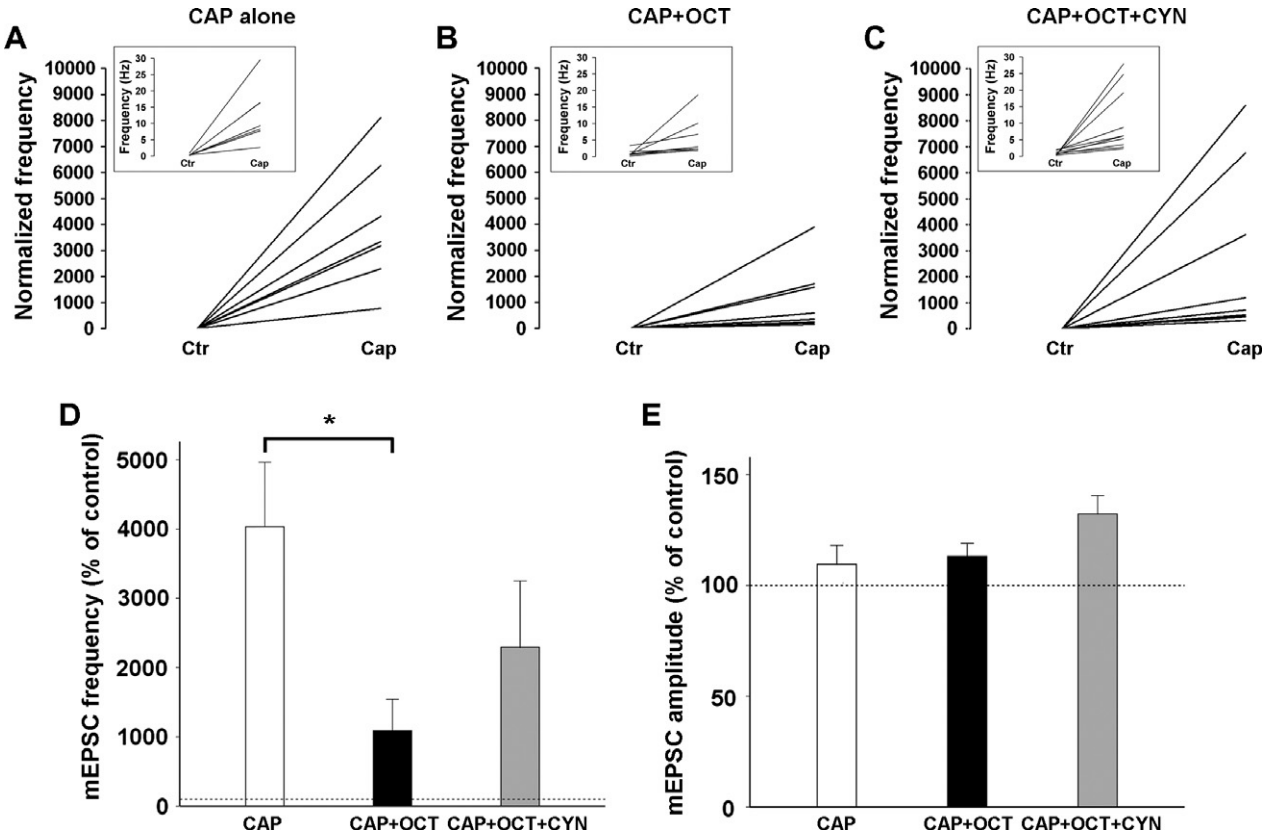

Fig. 2. OCT-mediated inhibition of CAP-induced mEPSC frequency increase. (A–C) Translation of mEPSCs frequency raw values (Hz, inset panels) in normalized values (% of control). Each line illustrates the CAP-induced frequency shift in single neurons under different experimental conditions (TTX in A, OCT in B and OCT + CYN 154806 in C). (D) mEPSC frequency increase in presence of CAP alone (white bar), CAP + OCT (black bars), and CAP + OCT + CYN 154806 (grey bars; Kruskal–Wallis test with Dunn's post hoc. *P < 0.05). (E) No differences were observed among mEPSC amplitudes (Kruskal–Wallis test with Dunn's post hoc. P > 0.05). Data are expressed as a percentage of the predrug control ± SEM. Dashed lines represent the control level. Abbreviations: CTR, control; CAP, capsaicin; OCT, octreotide; CYN, CYN 154806.

SSTR2a-immunoreactive axon terminals appeared in the form of C boutons in type Ia synaptic glomeruli (GIa; Ribeiro-da-Silva, 2004; Fig. 4A), and in non-glomerular configuration (Fig. 4B). In all SSTR2a-labelled pro- files, gold-intensified particles were localized along the plasma membrane, at synaptic and non-synaptic sites.
SSTR2a-immunopositive dendrites were typically contacted by unlabelled axonal terminals at conventional axo-dendritic synapses (Fig. 4C).
Quantitative ultrastructural analysis on a total of 160 profiles showed that, in P8-12 mice, the number of SSTR2a pre-synaptic profiles was 57.5% of total (of which 35% in type Ia glomeruli and 22.5% in non-glomerular axon terminals), while post-synaptic labelling in dendrites was 42.5%. No significant differences were observed in P21-23 mice (53.7% in axon terminals of which 38.7% type Ia glomeruli and 15% non-glomerular axon terminals; 46.3% in dendrites).
Finally, we performed a series of double immunolabelling experiments associating the fluoronanogold pre-embedding localization of SSTR2a with the post-embedding immunogold visualization of the IB4 binding sites. These experiments confirmed the light microscopy observations on the co-localization of SSTR2a and IB4, and, as an additional information, showed that co-expression only occurred in type Ia non-peptidergic glomeruli (Fig. 4D). In these preparations, both labels were localized over the plasma membrane, but were easily distinguishable. IB4 post-embedding immunolabelling was associated with the presence of gold particles of very regular round shapes and constant size (20 nm, see insert of Fig. 4D), while SSTR2a pre-embedding immunostaining was in the form of very electrondense particles of relatively large sizes (25–30 nm) and irregular shapes (insert of Fig. 4D).

3.3. OCT prevents the CAP-induced increase of Fos immunoreactivity in the superficial DH

The proto-oncogene c-fos is rapidly activated following membrane depolarization, and the protein Fos is largely used as a marker of neuronal activation (Morgan and Curran, 1991, 1995). Several observations in vivo have shown that Fos immunoreactivity is increased under different conditions of increased pain stimulation (see for example Coggeshall, 2005). We have previously demonstrated that Fos immunoreactivity is also increased in acute spinal cord slices when nociceptive PAFs are stimulated by CAP (Vergnano et al., 2008). Therefore, the effect of OCT on the CAP activation of nociceptive pathways at the DH level was further investigated by studying the c-fos response in vitro (Fig. 4). When slices were incubated with CAP, the number of Fos immunoreactive nuclei was increased in the superficial laminae of DH in comparison to controls (Fig. 4E and F). However, the Fos response was blocked when slices were incubated in the presence of CAP + OCT (Fig. 4G) and density of immunoreactive nuclei remained similar to that in controls (Fig. 4E). Statistic analysis confirmed the histological data: incubation with CAP (2 μM – 10 min) induced a significant increase of Fos

immunoreactivity in superficial DH (1382 ± 88 cells/mm^2, n = 50, Fig. 4H, black bar) compared to controls (902 ± 56 cells/mm^2, n = 38; one-way ANOVA, P < 0.001; Bonferroni post hoc test, P < 0.001, Fig. 4H, white bar). Notably, following pre-incubation with OCT (1 μM), the effect of CAP was largely prevented (914 ± 48 cells/mm^2, n = 49; Bonferroni post hoc, P < 0.001, Fig. 4H, grey bar).

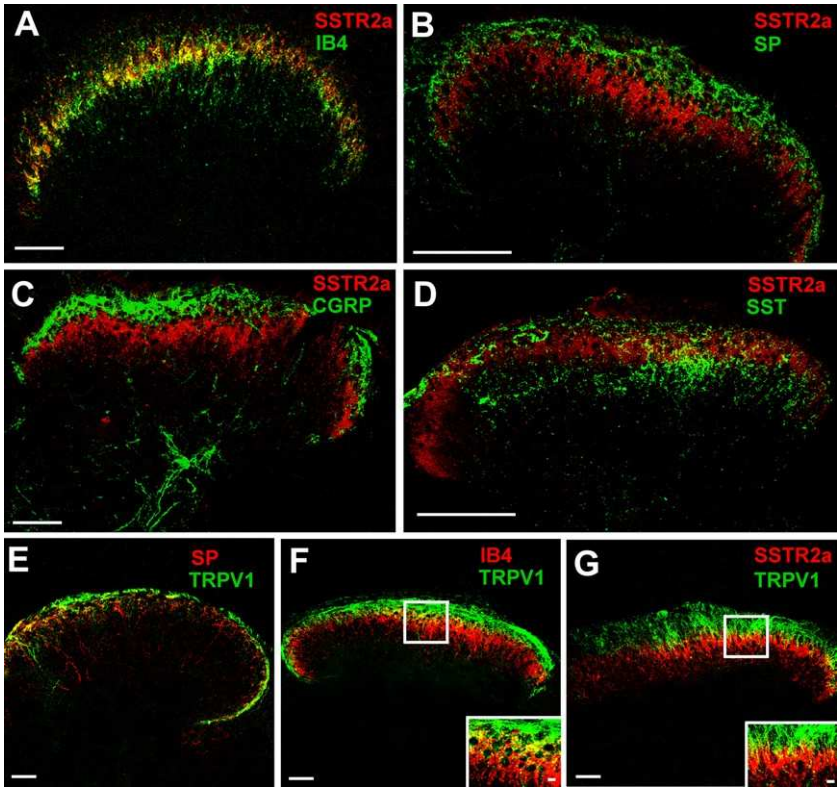

Fig. 3. Distribution of SSTR2a and co-localization with nociceptive PAF markers in spinal lamina II. A: SSTR2a (red) and IB4 (green) are extensively co-expressed (yellow) in nociceptive non-peptidergic primary afferent terminals of lamina II$_i$. (B) SSTR2a (red) and SP (green) are distributed in two different populations of PAFs, with SSTR2a principally distributed in lamina II$_i$ and SP in lamina I and lamina II$_o$. (C) SSTR2a (red) and CGRP (green) are localized in two different populations of PAFs. Labelling for CGRP is most pronounced in lamina I and II$_o$, whereas staining for SSTR2a is denser in lamina II$_i$. (D) staining for SSTR2a (red) and SST (green) only partly overlap (yellow) in lamina II$_o$. (E) SP (red) and TRPV1 (green) are co-expressed in a population of PAFs distributed in lamina I. (F) IB4 (red) and TRPV1 (green) are co-expressed in a population of PAFs distributed at the border between lamina I and lamina II$_o$. Labelling for IB4 is most pronounced in lamina II$_i$, whereas staining for TRPV1 is denser in lamina I. (G) SSTR2a (red) and TRPV1 (green) immunoreactivities are localized in a population of fibres at the border between lamina II$_o$ and lamina II$_i$. Scale bar: 200 μm.

4. Discussion

In the present study, we have shown that SSTRs2a are expressed by a population of TRPV1-positive non-peptidergic PAFs localized at the interface between lamina II$_o$

and II¡ of the spinal cord DH, and that pre-synaptic activation of these receptors produced a sig- nificant reduction of the CAP-induced release of glutamate from nociceptive PAFs.

4.1. Distribution of SSTR2a

The distribution of SSTR2a in rat DRGs and DH has been re- ported in several studies (Schulz et al., 1998a,b; Segond von Banchet et al., 1999; Bar et al., 2004; Carlton et al., 2004). Although the localization of SSTR2a in small to medium sized DRG neurons has been confirmed by different authors (Schulz et al., 1998b; Bar et al., 2004; Carlton et al., 2004), receptor localization in DH has been mainly described within neuronal processes and somata in lamina II. In addition, ultrastructural and dorsal rhizotomy studies have failed to demonstrate receptor expression in PAF central projections (Schulz et al., 1998a,b; Zhao et al., 2008).
This is the first report describing the expression of SSTR2a in mouse spinal cord. In this species, we observed, at the light micro- scope, the co-localization of SSTR2a and IB4 in fibres of spinal cord lamina II. Since IB4 is a marker of non-peptidergic nociceptive PAFs (Guo et al., 1999), the present study demonstrates that a specific sub-population of PAF central projections specifically express the SSTR2a. This observation was confirmed by: (i) the lack of co-localization between SSTR2a and SP/CGRP and (ii) the ultrastructural observation that about 60% of SSTR2a-immunoreactive profiles in lamina II were axon terminals, two thirds of them being the C boutons of type Ia non-peptidergic glomeruli (Ribeiro-da-Silva, 2004).

4.2. SSTR2a and TRPV1 receptors in spinal DH

At periphery, SSTRs2a are expressed on nociceptor terminals, and exert a tonic inhibitory control on the activation of the CAP receptor TRPV1 (Carlton et al., 2004). This effect likely involves a direct receptor interaction within the same nerve endings. We have here observed the co-expression of TRPV1 and SSTR2a in a subset of IB4-positive PAF central terminals, in keeping with the notion that even though TRPV1 is known to be mainly expressed in peptidergic PAFs (Cavanaugh et al., 2009), the receptor is also present and functional in a sub-population of IB4-positive fibres (Guo et al., 1999; Woodbury et al., 2004; Breese et al., 2005; Vil-ceanu et al., 2010).

4.3. Physiological relevance of SSTR2a and TRPV1 co-expression in lamina II

In spite of the robust expression of SSTRs at pre-synaptic sites in lamina II, previous studies have mainly reported the occurrence of post-synaptic inhibitory effects of SST in rat DH, but failed to detect significant SST-mediated pre-synaptic effects (Kim et al., 2002; Jiang et al., 2003).

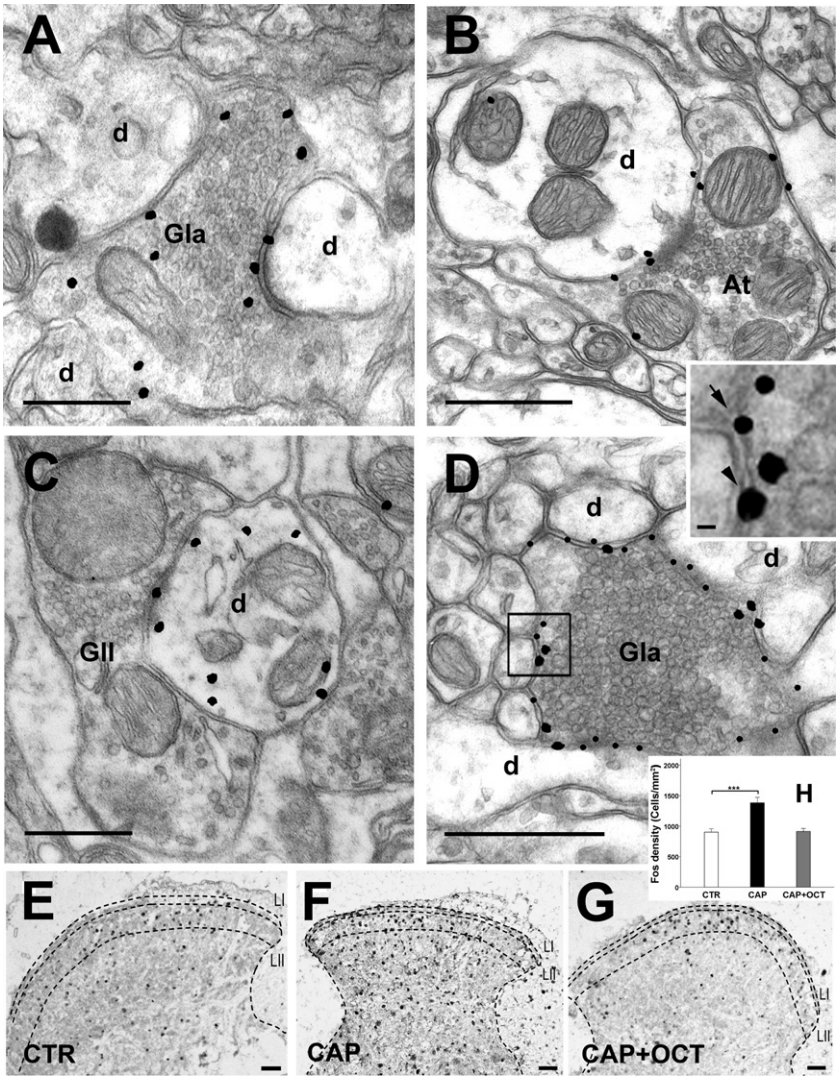

Fig. 4. Ultrastructural localization of SSTR2a in spinal lamina II and OCT inhibition of the CAP-induced Fos response in superficial DH. (A) A SSTR2a-immunoreactive type Ia glomerular terminal (GIa) is surrounded by several unlabelled dendrites (d). SSTR2a-labelling is characterized by irregular gold particles of large sizes, as a result of the gold- intensification procedure, and is prevalently distributed along the plasma membrane. (B) A SSTR2a-immunoreactive non-glomerular axon terminal (At) contacts an unlabelled dendrite (d). Gold particles are distributed over the plasma membrane, at both synaptic and non-synaptic sites. (C) A SSTR2a-labelled dendrite is post-synaptic to an unlabelled type II glomerular terminal (GII). SSTR2a gold-intensified particles are distributed along the plasma membrane. (D) A SSTR2a+IB4-immunoreactive type Ia glomerular terminal (GIa) is surrounded by several unlabelled dendrites (d). Both the labels are localized over the plasma membrane, but IB4 post-embedding immunolabelling is associated with the presence of gold particles of very regular round shapes and constant size (20 nm, arrows in the insert), while SSTR2a pre-embedding immunostaining appears in the form of electrondense particles of relatively large sizes (25–30 nm) and irregular shapes (arrowhead in the insert). (E–G) Fos immunoreactivity in superficial DH under CTR condition (E), after CAP administration (F), and after CAP administration in presence of OCT 1 μM (G). (H) Mean density of Fos immunoreactive nuclei observed in superficial DH under CTR condition (white bar) compared to CAP (black bar) and

CAP + OCT (grey bar) experiments (one-way ANOVA, Bonferroni post hoc, $P < 0.001$). A significant increase in cell density was observed after CAP, but not after CAP + OCT. $^{***}P < 0.001$. Abbreviations: CTR, control; CAP, capsaicin; OCT, octreotide; LI, lamina I; LII, lamina II; dashed lines indicate lamina I and II profiles. Scale bars: A–D = 500 nm; insert: 20 nm; E–G = 100 μm.

In the present study, we have used OCT, a more stable synthetic analogue of SST that is not degraded by cell peptidases so rapidly like SST and thus is more suitable for slice studies. In keeping with previous studies (Kim et al., 2002; Jiang et al., 2003), we have been unable to detect any relevant direct effect of OCT on either mIPSCs or mEPSCs in lamina II neurons (data not shown). However, the findings reported in this work demonstrate that pre-synaptic SSTRs2 have a role in the control of lamina II excitatory transmission that follows the activation of nociceptive PAFs by CAP. Our patch clamp experiments, in fact, were performed under conditions to pharmacologically isolate the pre-synaptic effects of OCT by the addition of a specific inhibitor to block the intracellular pathway related to G protein activation of SSTRs in recorded neurons. Although OCT is a high affinity agonist for SSTR2, SSTR3 and SSTR5 (Hannon et al., 2002), the main involve- ment of SSTR2 was confirmed in our experiments by using CYN 154806, a selective antagonist of this receptor subtype in mouse (Terashima et al., 2009; Cammalleri et al., 2004) and other species (see Section 2.1). CYN 154806 significantly blocked the inhibition exerted by OCT on the CAP-mediated increase of mEPSC frequency. Under these conditions, we also detected a slight mEPSC amplitude increase following CAP that was not observed in presence of CAP alone. This observation likely reflects the existence of a tonic SSTR2-mediated inhibitory activity on the pre-synaptic release of glutamate, which is removed when the receptor is blocked. In other words, under conditions of action potential block (such as it occurs in the presence of TTX) the more obvious explanation for the observed increase in mEPSC amplitude that follows a challenge with CAP + CYN 154806 (but not with CAP alone) is that SSTR2 is normally in a steady (tonic) state of activation in DH, and thus constantly reduces the glutamate release evoked by TRPV1. In keeping with these findings, previous studies suggested the existence of release-inhibiting SSTRs2 on central glutamatergic synapses that similarly affect K^+-evoked glutamate release (Grilli et al., 2004).

Although being specific for SSTR2, it seems unlikely that CYN 154806 is able to discriminate between SSTR2a and b, given that the latter is a truncated form of the receptor lacking about 300 nucleotides between transmembrane segment (TMS) VII and the C-terminus, and that peptide agonists (such as CYN 154806) tend to bind to epitopes evenly distributed along the exofacial regions, i.e., both the amino-terminal neck (ATN) and extracellular loops I–III (see Møller et al. (2003) for further discussion). Nonetheless, being SSTR2a the most prominent receptor subtype in rat nociceptive pathways, and given the specificity for SSTR2a of the primary antibody employed in this study (see Section 2.2), one can safely conclude

that effects mediated by OCT in electrophysiological experiments are indeed due to SSTR2a specific activation.

It is a common notion that the intense excitatory effects of CAP in DH are substantially consequence of strong glutamate release from TRPV1-expressing PAFs (Urban and Dray, 1992; Yang et al., 1998). Under inflammatory conditions in vivo (Zhang et al., 1998) this is followed by c-fos activation of DH neurons. In a different experimental paradigm in vitro, i.e. the acute spinal cord slice, we have previously demonstrated that CAP stimulation of nociceptive PAFs up-regulates Fos expression in DH (Vergnano et al., 2008). Such a type of response indicates that at the CAP concentration used in our studies, challenge of acute spinal cord slices mimics an inflammatory condition in vitro.

In the present work, OCT produced a significant reduction of CAP-induced Fos expression in superficial laminae of DH. Whereas the OCT-mediated reduction of CAP-induced mEPSC frequency in- crease was about 70%, OCT almost completely blocked the CAP response as measured in terms of Fos immunoreactivity. This apparent discrepancy is likely due to the contribution of both pre- and post-synaptic SSTR2a in c-fos experiments. Nonetheless, these observations indicate that activation of SSTR2a in non-peptidergic nociceptive PAFs may also be of relevance for modulation of the inflammatory response in vivo, given that SST is physiologically present in DH.

We have chosen to evaluate the SSTR2a central response to OCT in a slice inflammatory pain model since numerous preclinical and clinical studies have implicated SSTR2 in the response to peripheral inflammation (see for example Ji et al., 2006; Paran et al., 2001, 2005), and SST is widely recognized as an endogenous anti-inflammatory peptide (see Malcangio, 2003). Nonetheless, SST has been also linked to the onset of neuropathic pain (Dong et al., 2006; Adler et al., 2009), mainly in response to glial cell-line derived neurotrophic factor (GDNF) stimulation. It would be of interest in future experiments to assess the involvement of SSTR2a in neuropathic pain. However, given the availability of a limited number of selective compounds that may be suitable for central studies this might prove a very hard task.

4.4. **SST in DH**

While previous studies indicated that SST and SST agonists have little effects on resting synaptic transmission and transmitter release in vitro (Kim et al., 2002; Jiang et al., 2003), our present observations suggest that OCT inhibits glutamate neurotransmission following an intense stimulation of nociceptive pathways. These data are consistent with the observation that SST is antinociceptive in pathological pain (Malcangio, 2003; Pintér et al., 2006). The comprehension of the role of SST in pain processing mechanisms is complicated by the existence of several SST sources in spinal cord, i.e. the PAFs, the DH interneurons and the descending projections (see Malcangio (2003) for review). Our data demonstrate

the existence of a specific SSTR2a-mediated pre-synaptic mechanism involved in the control of the TRPV1 central effects at the level of non-peptidergic PAFs. In chronic or pathological pain, the central re- lease of SST can be increased, as inferred from the rise of SST in cerebro-spinal fluid (Unger et al., 1988). Under these conditions, and in line with our present findings, SST may reach a local concentration in DH sufficiently high to activate the SSTR2a expressed by the non-peptidergic central terminals of PAFs, eventually limiting the excitatory or neurotoxic effects of the massive release of glutamate that occurs as a consequence of an intense nociceptive stimulation.

4.5. Conclusions

SST has been proved to modulate the activity of sensory neurons (Malcangio, 2003) and its synthetic analogue OCT has recently gained increasing attention in the clinical treatment of chronic and cancer pain (Schwetz et al., 2004; Newsome et al., 2008; Gachago and Draganov, 2008), but the mechanisms underlying its effects are still largely obscure. In animal models, OCT anti-hyperalgesic effects were mainly observed following intrathecal administration (Su et al., 2001), suggesting the involvement of spinal rather than peripheral mechanisms. From the present study, it derives that OCT effects are for the most due to interplay with TRPV1s at lamina II synapses. We have recently demonstrated that, upon activation of central TRPV1s in peptidergic nociceptive PAFs, a relevant parallel pathway independent from glutamate transmits nociceptive information to lamina II neurons (Ferrini et al., 2007). We demonstrate here that activation of non-peptidergic nociceptive PAFs expressing TRPV1s is an additional pathway to modulate glutamate release in inflammatory conditions. Therefore, our study fur- ther supports the efficacy of OCT in reducing pain transmission at the spinal DH level.

Acknowledgements

This work was supported by the Italian MiUR (Fondi PRIN 2008) and Compagnia di San Paolo Torino.

References

Adler JE, Nico L, VandeVord P, Skoff AM. Modulation of neuropathic pain by a glial- derived factor. Pain Med 2009;10:1229–36.

Bar KJ, Schurigt U, Scholze A, Segond Von Banchet G, Stopfel N, Brauer R, et al. The expression and localization of somatostatin receptors in dorsal root ganglion neurons of normal and monoarthritic rats. Neuroscience 2004;127:197–206.

Baumeister H, Kreuzer OJ, Roosterman D, Schäfer J, Meyerhof W. Cloning, expression, pharmacology and tissue distribution of the mouse somatostatin receptor subtype 5. J Neuroendocrinol 1998;10:283–90.

Breese NM, George AC, Pauers LE, Stucky CL. Peripheral inflammation selectively increases TRPV1 function in IB4-positive sensory neurons from adult mouse. Pain 2005;115:37–49.

Cammalleri M, Cervia D, Langenegger D, Liu Y, Dal Monte M, Hoyer D, et al. Somatostatin receptors differentially affect spontaneous epileptiform activity in mouse hippocampal slices. Eur J Neurosci 2004;10:2711–21.

Carlton SM, Du J, Zhou S, Coggeshall RE. Tonic control of peripheral cutaneous nociceptors by somatostatin receptors. J Neurosci 2001;21:4042–9.

Carlton SM, Zhou S, Du J, Hargett GL, Ji G, Coggeshall RE. Somatostatin modulates the transient receptor potential vanilloid 1 (TRPV1) ion channel. Pain 2004;110:616–27.

Caterina MJ, Schumacher MA, Tominaga M, Rosen TA, Levine JD, Julius D. The capsaicin receptor: a heat-activated ion channel in the pain pathway. Nature 1997;389:816–24.

Cavanaugh DJ, Lee H, Lo L, Shields SD, Zylka MJ, Basbaum AI, et al. Distinct subsets of unmyelinated primary sensory fibers mediate behavioral responses to noxious thermal and mechanical stimuli. Proc Natl Acad Sci USA 2009;106:9075–80.

Coggeshall RE. Fos, nociception and the dorsal horn. Prog Neurobiol 2005;77:299–352.

Dahaba AA, Mueller G, Mattiassich G, Rumpold-Seitlinger G, Bornemann H, Rehak PH, et al. Effect of somatostatin analogue octreotide on pain relief after major abdominal surgery. Eur J Pain 2009;13:861–4.

Dong ZQ, Wang YQ, Ma F, Xie H, Wu GC. Down-regulation of GFRa-1 expression by antisense oligodeoxynucleotide aggravates thermal hyperalgesia in a rat model of neuropathic pain. Neuropharmacology 2006;50:393–403.

Feniuk W, Jarvie E, Luo J, Humphrey PP. Selective somatostatin sst2 receptor blockade with the novel cyclic octapeptide, CYN-154806. Neuropharmacology 2000;39:1443–50.

Ferrini F, Salio C, Vergnano AM, Merighi A. Vanilloid receptor-1 (TRPV1)-dependent activation of inhibitory neurotransmission in spinal substantia gelatinosa neurons of mouse. Pain 2007;129:195–209.

Ferrini F, Salio C, Lossi L, Gambino G, Merighi A. Modulation of inhibitory neurotransmission by the vanilloid receptor type 1 (TRPV1) in organotypically cultured mouse substantia gelatinosa neurons. Pain 2010;150:128–40.

Fitzgerald M. The development of nociceptive circuits. Nat Rev Neurosci 2005;6:507–20.

Gachago C, Draganov PV. Pain management in chronic pancreatitis. World J Gastroenterol 2008;14:3137–48.

Grilli M, Raiteri L, Pittaluga A. Somatostatin inhibits glutamate release from mouse cerebrocortical nerve endings through presynaptic sst2 receptors linked

to the adenylyl cyclase-protein kinase A pathway. Neuropharmacology 2004;46:388–96.

Guo A, Simone DA, Stone LS, Fairbanks CA, Wang J, Elde R. Developmental shift of vanilloid receptor 1 (VR1) terminals into deeper regions of the superficial dorsal horn: correlation with a shift from TrkA to Ret expression by dorsal root ganglion neurons. Eur J Neurosci 2001;14:293–304.

Guo A, Vulchanova L, Wang J, Li X, Elde R. Immunocytochemical localization of the vanilloid receptor 1 (VR1): relationship to neuropeptides, the P2X3 purinoceptor and IB4 binding sites. Eur J Neurosci 1999;11:946–58.

Hannon JP, Nunn C, Stolz B, Bruns C, Weckbecker G, Lewis I, et al. Drug design at peptide receptors: somatostatin receptor ligands. J Mol Neurosci 2002;18:15–27.

Ji GC, Zhou ST, Shapiro G, Reubi JC, Jurczyk S, Carlton SM. Analgesic activity of a non- peptide imidazolidinedione somatostatin agonist: in vitro and in vivo studies in rat. Pain 2006;124:34–49.

Jiang N, Furue H, Katafuchi T, Yoshimura M. Somatostatin directly inhibits substantia gelatinosa neurons in adult rat spinal dorsal horn in vitro. Neurosci Res 2003;47:97–107.

Kim SJ, Chung WH, Rhim H, Eun SY, Jung SJ, Kim J. Postsynaptic action mechanism of somatostatin on the membrane excitability in spinal substantia gelatinosa neurons of juvenile rats. Neuroscience 2002;114:1139–48.

Malcangio M, Getting SJ, Grist J, Cunningham JR, Bradbury EJ, Charbel Issa P, et al. A novel control mechanism based on GDNF modulation of somatostatin release from sensory neurones. FASEB J 2002;16:730–2.

Malcangio M. GDNF and somatostatin in sensory neurones. Curr Opin Pharmacol 2003;3:41–5.

Merighi A, Polak JM, Fumagalli G, Theodosis DT. Ultrastructural localization of neuropeptides and GABA in rat dorsal horn: a comparison of different immunogold labeling techniques. J Histochem Cytochem 1989;37: 529–40.

Merighi A, Polak JM, Theodosis DT. Ultrastructural visualization of glutamate and aspartate immunoreactivities in the rat dorsal horn, with special reference to the co-localization of glutamate, substance P and calcitonin-gene related peptide. Neuroscience 1991;40:67–80.

Michael GJ, Priestley JV. Differential expression of the mRNA for the vanilloid receptor subtype 1 in cells of the adult rat dorsal root and nodose ganglia and its downregulation by axotomy. J Neurosci 1999;19:1844–54.

Molander C, Xu Q, Grant G. The cytoarchitectonic organization of the spinal cord in the rat. I. The lower thoracic and lumbosacral cord. J Comp Neurol 1984;230:133–41.

Møller LN, Stidsen CE, Hartmann B, Holst JJ. Somatostatin receptors. Biochim Biophys Acta 2003;1616:1–84.

Morgan JI, Curran T. Stimulus-transcription coupling in the nervous system:

involvement of the inducible proto-oncogenes fos and jun. Annu Rev Neurosci 1991;14:421–51.

Morgan JI, Curran T. Immediate-early genes: ten years on. Trends Neurosci 1995;18:66–7.

Mori K, Kim J, Sasaki K. Electrophysiological effect of ghrelin and somatostatin on rat hypothalamic arcuate neurons in vitro. Peptides 2010;31:1139–45.

Newsome S, Frawley BK, Argoff CE. Intrathecal analgesia for refractory cancer pain. Curr Pain Headache Rep 2008;12:249–56.

Olias G, Viollet C, Kusserow H, Epelbaum J, Meyerhof W. Regulation and function of somatostatin receptors. J Neurochem 2004;89:1057–91.

Paice JA, Penn RD, Kroin JS. Intrathecal octrotide for relief of intractable nonmalignant pain: 5-year experience with two cases. Neurosurgery 1996;38:203–7.

Paran D, Elkayam O, Mayo A, Paran H, Amit M, Yaron M, et al. A pilot study of a long acting somatostatin analogue for the treatment of refractory rheumatoid arthritis. Ann Rheum Dis 2001;60:888–91.

Paran D, Kidron D, Mayo A, Ziv O, Chowers Y, Caspi D, et al. Somatostatin analogue treatment attenuates histological findings of inflammation and increases mRNA expression of interleukin-1 beta in the articular tissue of rats with ongoing adjuvant-induced arthritis. Rheumatol Int 2005;25:350–6.

Patel YC, Srikant CB. Somatostatin receptors. Trends Endocrinol Metab 1997;8: 398–405.

Patel YC. Somatostatin and its receptor family. Front Neuroendocrinol 1999;20:157–98.

Paxinos G, Watson C. The rat brain in stereotaxic coordinates. 4th ed. Sydney: Academic Press; 1998.

Penn RD, Paice JA, Kroin JS. Octreotide: a potent new non-opiate analgesic for intrathecal infusion. Pain 1992;49:13–9.

Pintér E, Helyes Z, Szolcsányi J. Inhibitory effect of somatostatin on inflammation and nociception. Pharmacol Ther 2006;112:440–56.

Ribeiro-da-Silva A. Substantia gelatinosa of spinal cord. In: Paxinos G, editor. The rat nervous system. Sydney: Academic Press; 2004.

Salio C, Lossi L, Ferrini F, Merighi A. Ultrastructural evidence for a pre-and postsynaptic localization of full-length trkB receptors in substantia gelatinosa (lamina II) of rat and mouse spinal cord. Eur J Neurosci 2005;22:1951–66.

Schulz S, Händel M, Schreff M, Schmidt H, Höllt V. Localization of five somatostatin receptors in the rat central nervous system using subtype-specific antibodies. J Physiol 2000;94:259–64.

Schulz S, Schmidt H, Händel M, Schreff M, Höllt V. Differential distribution of alternatively spliced somatostatin receptor 2 isoforms (sst2A and sst2B) in rat spinal cord. Neurosci Lett 1998a; 257:37–40.

Schulz S, Schreff M, Schmidt H, Händel M, Przewlocki R, Höllt V. Immunocytochemical localization of somatostatin receptor sst2A in the rat spinal cord and dorsal root ganglia. Eur J Neurosci 1998b;12:3700–8.

Schwabe W, Brennan MB, Hochgeschwender U. Isolation and characterization of the mouse (Mus musculus) somatostatin receptor type-4-encoding gene (mSSTR4). Gene 1996;168:233–5.

Schwetz I, Naliboff B, Munakata J, Lembo T, Chang L, Matin K, et al. Anti-hyperalgesic effect of octreotide in patients with irritable bowel syndrome. Aliment Pharmacol Ther 2004;19:123–31.

Segond von Banchet G, Schindler M, Hervieu GJ, Beckmann B, Emson PC, Heppelmann B. Distribution of somatostatin receptor subtypes in rat lumbar spinal cord examined with gold-labelled somatostatin and anti-receptor antibodies. Brain Res 1999;816:254–7.

Selmer IS, Schindler M, Allen JP, Humphrey P, Emson PC. Advances in understanding neuronal somatostatin receptors. Regul Pept 2000;90:1–18.

Señaris RM, Schindler M, Humphrey PPA, Emson PC. Expression of somatostatin receptor 3 mRNA in the motorneurones of the rat spinal cord, and the sensory neurones of the spinal ganglia. Brain Res Mol Brain Res 1995;29:185–90.

Su X, Burton MB, Gebhart GF. Effects of octreotide on responses to colorectal distension in the rat. Gut 2001;48:676–82.

Takeda M, Kadoi J, Takahashi M, Nasu M, Matsumoto S. Somatostatin inhibits the excitability of rat small-diameter trigeminal ganglion neurons that innervate nasal mucosa and project to the upper cervical dorsal horn via activation of somatostatin 2a receptor. Neuroscience 2007;148:744–56.

Terashima S, Nishio H, Ogura M, Honda M, Takeuchi K. Involvement of prostacyclin/ IP receptors in decreased acid response of damaged stomachs-mediation by somatostatin/SST 2 receptors. Life Sci 2009;84:172–80.

Tominaga M, Caterina MJ, Malberg AB, Rosen TA, Gilbert H, Skinner K, et al. The cloned capsaicin receptor integrates multiple pain-producing stimuli. Neuron 1998;21:531–43.

Urban L, Dray A. Synaptic activation of dorsal horn neurons by selective C-fibre excitation with capsaicin in the mouse spinal cord in vitro. Neuroscience 1992;47:693–702.

Unger J, Weindl A, Ochs G, Struppler A. CSF somatostatin is elevated in patients with postzoster neuralgia. Neurology 1988;38:1423–7.

Vergnano AM, Ferrini F, Salio C, Lossi L, Baratta M, Merighi A. The gastrointestinal hormone ghrelin modulates inhibitory neurotransmission in deep laminae of mouse spinal cord dorsal horn. Endocrinology 2008;149:2306–12.

Vilceanu D, Honore P, Hogan QH, Stucky CL. Spinal nerve ligation in mouse upregulates TRPV1 heat function in injured IB4-positive nociceptors. J Pain

2010;11:588–99.
Viollet C, Lepousez G, Loudes C, Videau C, Simon A, Epelbaum J. Somatostatinergic systems in brain. Networks and functions. Mol Cell Endocrinol 2008;286:75–87.
Viollet C, Prévost G, Maubert E, Faivre-Bauman A, Gardette R, kordon C, et al. Molecular pharmacology of somatostatin receptors. Fundam Clin Pharmacol 1995;9:107–13.
Woodbury CJ, Zwick M, Wang S, Lawson JJ, Caterina MJ, Koltzenburg M, et al. Nociceptors lacking TRPV1 and TRPV2 have normal heat responses. J Neurosci 2004;24:6410–5.
Yamada Y, Post SR, Wang K, Tager HS, Bell GI, Seino S. Cloning and functional characterization of a family of human and mouse somatostatin receptors expressed in brain, gastrointestinal tract and kidney. Proc Natl Acad Sci USA 1992;89:251–5.
Yang K, Kumamoto E, Furue H, Yoshimura M. Capsaicin facilitates excitatory but not inhibitory synaptic transmission in substantia gelatinosa of the rat spinal cord. Neurosci Lett 1998;255:135–8.
Yasuda K, Rens-Domiano S, Breder CD, Law SF, Saper CB, Reisine T, et al. Cloning of a novel somatostatin receptor, SSTR3, coupled to adenylylcyclase. J Biol Chem 1992;267:20422–8.
Zhang RX, Wang H, Ruda M, Iadarola MJ, Qiao JT. c-Fos expression in NMDA receptor-contained neurons in spinal cord in a rat model of inflammation: a double immunocytochemical study. Brain Res 1998;795:282–6.
Zhao J, Hu JY, Zhang YQ, Zhao ZQ. Involvement of spinal somatostatin receptor SST(2A) in inflammation-induced thermal hyperalgesia: ultrastructural and behavioral studies in rats. Neurochem Res 2008;33:2099–106.